Computationally-efficient aeroelastic analysis tool for short-wing / propeller configuration on compound helicopters

Z. Wang [1], **A. A. Popov** [1]
[1] Department of Mechanical, Materials and Manufacturing Engineering,
University Park, University of Nottingham, Nottingham, United Kingdom
e-mail: **Zi.Wang@nottingham.ac.uk**

Abstract

A time-domain aeroelastic analysis for short-wing/propeller configuration in compound helicopters is presented in this paper. A linear Timoshenko beam is used in conjunction with analytical aerodynamic theories, while propeller effects are simplified as defined velocity profiles in the advancing and vertical directions. A numerical modal analysis approach is used to incorporate the coupling between bending and torsion. The paper focuses on the application of coupled mode shapes and Timoshenko beam in an aeroelasticity context. A Eurocopter X3-liked short-wing/propeller configuration is studied. Differences introduced by coupled mode shapes and Timoshenko beam theory are discussed. The results show that coupled modal analysis gives a better representation of the modal behaviour with less computational power required. While rotary inertia and shear deformation effects result in a higher mean deflection and a smaller amplitude in the steady state, revealing a different energy distribution mechanism compare to Euler-Bernoulli beam in the system studied.

1 Introduction

A major and still open issue in rotorcraft design is the high level of vibration resulting from the complex interaction between the main rotor and other structures. This interaction strongly affects the fatigue life of structures, maintenance costs, on-board instrumentation efficiency, and comfort. In the cases of compound helicopters and tilt-rotor aircraft, the vibrational behaviour is further complicated by the presence of fixed wings with propellers, or lateral rotors attached to the wing main structure. Another distinctive feature of these types of rotorcraft is the necessity to deliver rotational power to all rotors by the transmission systems which further influences the overall structural behaviour with their own dynamics.

The initiative of this paper is to disclose the scientific background of such complex aeroelastic behaviour using simple and numerically efficient models, which can be further implemented into design and optimisation stages for compound helicopter wing structures. The paper focuses on the application of coupled modal analysis and Timoshenko beam theory for aeroelastic response of short-wing/propeller configuration on compound helicopters.

The aeroelastic behaviour is governed by the structural dynamics and aerodynamic loadings of the wing-propeller system. To achieve the aim, the wing semi-span is simplified as a cantilever beam with a tip loaded propeller. Having to provide lift, secure tractor propellers in place and still maintain the compatibility of existing helicopter facilities, the wing needs to be a stiff and short one. Effects of shear deformations need to be taken into account in this case. Hence, a linear model based on the Timoshenko beam theory is used for characterising the wing's structural behaviour.

Studies using Euler-Bernoulli beam theory is a much more common topic in the area of aeroelasticity. As classic fixed-wing aircraft features a much slender wing, Euler-Bernoulli beam theory is usually sufficient enough [1–6]. For rotorcrafts, rotor blades are also slender structures that can be characterised by Euler-Bernoulli beam theory [7, 8]. There are some, however, limited cases featuring other beam theories when

studying aeroelastic systems. Application of a quasi-slender Rayleigh beam into a semi-analytical model was carried out by Berci et al. in [9]. Kämpchen et al. studied the aeroelastic response of a very elastic wing [10]. In his case, Timoshenko beam was used to avoid any energy dispersion by coupling between bending and translational motions. For short wings on compound helicopters, Timoshenko beam incorporating shear deformation effects is much more suitable.

For the aerodynamic loadings, predictions are made based on time-domain analytical sectional theories, such as the Wagner's and Küssner's models. In this particular case, the propeller slipstream effects on the wing are modelled as additional velocity components in the vertical and axial directions. Finally, by integrating the structural and aerodynamic models, the governing equations of motion for the short-wing and propeller system can be obtained. At this stage, only flapping and torsional motion are taken into account.

A numerical modal analysis approach is used to incorporate coupling between bending and torsion. Cantilever beam with coupled bending-torsion motion has been studied by Banerjee et al. [11–13]. They developed the analytical coupled modal frequencies and shapes for Euler-Bernoulli and Timoshenko beams, also stating that the application of coupled modes can be further used for aeroelasticity problems for better accuracy with less computational efforts. In the current paper, a numerical model based on transfer matrix method will be introduced and applied in an aeroelasticity context.

Based on the coupled mode shapes, the complete aeroelastic model can be discretised by Galerkin's method and solved numerically by Newmark-beta algorithm. An approach described in [14, 15] is used. The capability of the complete model is shown through a case study in similar configuration to Eurocopter X3. The aeroelastic responses will be compared to the ones obtained by uncoupled mode shapes and Euler-Bernoulli beam theory, respectively.

2 Mathematical model

2.1 Timoshenko beam theory

In the early 20th century, Timoshenko derived a beam theory that considers shear deformation and rotary inertia effects for thick/short beams [16, 17]. While an Euler-Bernoulli beam assumed slenderness and cross-section being planar and normal to the neutral axis, a Timoshenko beam allows shear deformation between beam cross-section and the neutral axis. For compound helicopters having fixed-wing features and tip-mounted propellers, the wing is a short one for the purpose of providing lift, securing propellers in place while still maintaining the compatibility with existing helicopter facilities. Therefore, the Euler-Bernoulli beam assumption for being slender is not valid. Instead a linear Timoshenko beam, in this case, can give a much more accurate representation for short and stiff wings in compound helicopters.

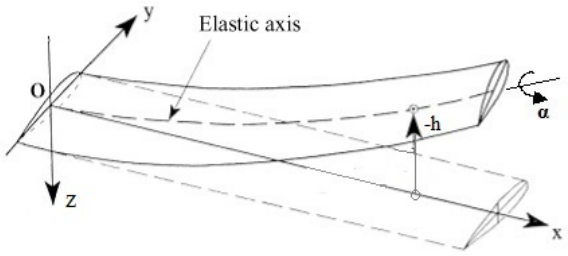

Figure 1: Beam model xyz coordinate

For a Timoshenko beam considering flapping (h) and torsional (α) motion as illustrated in Figure 1, its

governing equations can be written as

$$\begin{aligned} &m\frac{\partial^2 h}{\partial t^2} - mx_\alpha \frac{d^2\alpha}{dt^2} - \frac{\partial}{\partial x}[\kappa_h GA(\frac{\partial h}{\partial x} - \varphi_h)] = L_h \\ &\rho_w I_y \frac{\partial^2 \varphi_h}{\partial t^2} - \frac{\partial}{\partial x}(EI_y \frac{\partial \varphi_h}{\partial x}) - \kappa_h GA(\frac{\partial h}{\partial x} - \varphi_h) = 0 \\ &I_\alpha \frac{\partial^2 \alpha}{\partial t^2} - mx_\alpha \frac{\partial^2 h}{\partial t^2} - \frac{\partial}{\partial x}(GJ\frac{\partial \alpha}{\partial x}) = M_\alpha \end{aligned} \tag{1}$$

Where m is the mass per span, x_α is the distance between gravitational and shear centres, κ_h is the shear coefficient, E and G are the Young's and shear moduli, respectively, A is the cross-sectional area, φ_h is the sectional rotation allowing shear deformations, ρ_w is the wing's material density, I_y is the second moment of area, I_α is the mass moment of inertia per span, J is the torsional coefficient and L_h, M_α are the loadings in flapping and torsional coordinates.

Dimensionless time ($\tau = U_\infty t/b$) domain is used for this simulation by modifying the real time with the aircraft advancing speed U_∞ and half chord length b. Therefore, Equation (1) can be rewritten considering dimensionless bending displacement ($\xi = h/b$) as

$$\begin{aligned} &m\frac{U_\infty^2}{b}\ddot{\xi} - mx_\alpha \frac{U_\infty^2}{b^2}\ddot{\alpha} - [\kappa_h GA(b\xi' - \varphi_h)]' = L_h \\ &\rho_w I_y \frac{U_\infty^2}{b^2}\ddot{\varphi}_h - (EI_y\varphi_h')' - \kappa_h GA(b\xi' - \varphi_h) = 0 \\ &I_\alpha \frac{U_\infty^2}{b^2}\ddot{\alpha} - mx_\alpha \frac{U_\infty^2}{b}\ddot{\xi} - (GJ\alpha')' = M_\alpha \end{aligned} \tag{2}$$

Note that $\ddot{\xi}$, $\ddot{\alpha}$ and $\ddot{\varphi}_h$ are derivatives with respect to dimensionless time τ, while ξ', φ_h' and α' are derivatives with respect to wing span coordinate x.

Using modal analysis techniques, displacements in flapping and torsion can be rewritten as Equation (3). In the case studied, coupling between these two motions are involved. Therefore, coupled mode shapes are characterised through the transfer matrix method. Hence, they share the same time-dependent function $q_j(\tau)$.

$$\xi = \sum_{j=0}^{\infty} \theta_j(x) q_j(\tau); \qquad \varphi_h = \sum_{j=0}^{\infty} \phi_j(x) q_j(\tau); \qquad \alpha = \sum_{j=0}^{\infty} \eta_j(x) q_j(\tau); \tag{3}$$

2.1.1 Numerical modal analysis

To perform modal analysis, a numerical approach is introduced here. Comparing to theoretical expressions, this is a much more versatile way to obtain natural frequencies and mode shapes for structures with coupled motions. Simple harmonic motions for bending and torsion are assumed as

$$\xi = \sum_{j=0}^{\infty} \theta_j(x) e^{i\omega_j t}; \qquad \varphi_h = \sum_{j=0}^{\infty} \phi_j(x) e^{i\omega_j t}; \qquad \alpha = \sum_{j=0}^{\infty} \eta_j(x) e^{i\omega_j t}; \tag{4}$$

Therefore, with uniform beam properties, the governing equations of motion can be written as

$$\begin{aligned} &- mb\omega_j^2\theta_j + mx_\alpha\omega_j^2\eta_j - \kappa_h GA(b\theta_j'' - \phi_j') = 0 \\ &- \rho_w I_y\omega_j^2\phi_j - EI_y\phi_j'' - \kappa_h GA(b\theta_j' - \phi_j) = 0 \\ &- I_\alpha\omega_j^2\eta_j + mbx_\alpha\omega_j^2\theta_j - GJ\eta_j'' = 0 \end{aligned} \tag{5}$$

In general matrix form, Equation (5) can be rearranged as

$$\begin{Bmatrix} \theta_j' \\ \theta_j'' \\ \phi_j' \\ \phi_j'' \\ \eta_j' \\ \eta_j'' \end{Bmatrix} = \begin{bmatrix} 0 & 1 & 0 & 0 & 0 & 0 \\ -\frac{m\omega_j^2}{\kappa_h GA} & 0 & 0 & \frac{1}{b} & \frac{mx_\alpha\omega_j^2}{\kappa_h GAb} & 0 \\ 0 & 0 & 0 & 1 & 0 & 0 \\ 0 & -\frac{\kappa_h GAb}{EI_y} & \frac{\kappa_h GA - \rho_w I_y \omega_j^2}{EI_y} & 0 & 0 & 0 \\ 0 & 0 & 0 & 0 & 0 & 1 \\ \frac{mx_\alpha\omega_j^2}{GJ} & 0 & 0 & 0 & -\frac{I_\alpha\omega_j^2}{GJ} & 0 \end{bmatrix} \begin{Bmatrix} \theta_j \\ \theta_j' \\ \phi_j \\ \phi_j' \\ \eta_j \\ \eta_j' \end{Bmatrix} = \mathbf{A} \begin{Bmatrix} \theta_j \\ \theta_j' \\ \phi_j \\ \phi_j' \\ \eta_j \\ \eta_j' \end{Bmatrix} \tag{6}$$

Therefore,

$$\left\{\theta_j(x)\ \theta_j'(x)\ \phi_j(x)\ \phi_j'(x)\ \eta_j(x)\ \eta_j'(x)\right\}^{\mathrm{T}} = e^{\mathbf{A}x} \left\{\theta_j(0)\ \theta_j'(0)\ \phi_j(0)\ \phi_j'(0)\ \eta_j(0)\ \eta_j'(0)\right\}^{\mathrm{T}} \tag{7}$$

To implement boundary conditions, the displacement parameters can be corrected into loading/displacement parameters as

$$\begin{Bmatrix} \theta_j(x) \\ S(x) \\ \phi_j(x) \\ M(x) \\ \eta_j(x) \\ T(x) \end{Bmatrix} = \begin{bmatrix} 1 & 0 & 0 & 0 & 0 & 0 \\ 0 & \kappa_h GAb & -\kappa_h GA & 0 & 0 & 0 \\ 0 & 0 & 1 & 0 & 0 & 0 \\ 0 & 0 & 0 & -EI_y & 0 & 0 \\ 0 & 0 & 0 & 0 & 1 & 0 \\ 0 & 0 & 0 & 0 & 0 & GJ \end{bmatrix} \begin{Bmatrix} \theta_j(x) \\ \theta_j'(x) \\ \phi_j(x) \\ \phi_j'(x) \\ \eta_j(x) \\ \eta_j'(x) \end{Bmatrix} = \mathbf{D} \begin{Bmatrix} \theta_j(x) \\ \theta_j'(x) \\ \phi_j(x) \\ \phi_j'(x) \\ \eta_j(x) \\ \eta_j'(x) \end{Bmatrix} \tag{8}$$

For cantilever beams, boundary conditions write as

Table 1: Cantilever beam boundary conditions

Root condition	$\theta_j(0) = 0$	$\phi_j(0) = 0$	$\eta_j = 0$
Tip condition	$S(l) = 0$	$M(l) = 0$	$T(l) = 0$

With boundary conditions applied to both ends of the beam, Equation (8) becomes

$$\begin{Bmatrix} S(l) = 0 \\ M(l) = 0 \\ T(l) = 0 \end{Bmatrix} = \mathbf{T}\mathbf{D}e^{\mathbf{A}l}\mathbf{D}^{-1}\mathbf{R} \begin{Bmatrix} S(0) \\ M(0) \\ T(0) \end{Bmatrix} \quad \text{where} \quad \mathbf{T} = \begin{bmatrix} 0 & 1 & 0 & 0 & 0 & 0 \\ 0 & 0 & 0 & 1 & 0 & 0 \\ 0 & 0 & 0 & 0 & 0 & 1 \end{bmatrix} \ ; \ \mathbf{R} = \mathbf{T}' \tag{9}$$

By solving the zero determinant of $\det(\mathbf{T}\mathbf{D}e^{\mathbf{A}l}\mathbf{D}^{-1}\mathbf{R})$, coupled natural frequencies and mode shapes can be obtained.

2.2 Aerodynamic Loadings

The unsteady aerodynamic loadings are characterised through analytical theories. The same approach was developed and used in [14, 15], featuring the Wagner's and Küssner's functions. As illustrated in Figure 2, the aerodynamic loadings consist of circulatory terms (L_C, M_C) and non-circulatory terms (L_{NC}, M_{NC}).

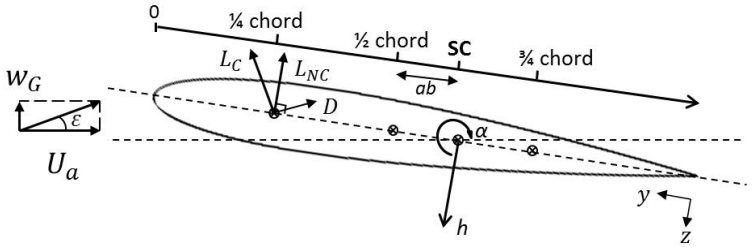

Figure 2: Aerofoil notation

Wagner discovered that the circulatory lift can be formulated in dimensionless time domain as a function of downwash induced at 3/4 chord $w_{3/4}$ [18]. Therefore, it writes

$$\begin{gathered} L_C = -2\pi b\rho U_a \phi(\tau) w_{3/4}(0) - 2\pi b\rho U_a \int_0^\tau \phi(\tau-\tau_0) w_{3/4}(\tau_0) d\tau_0 \quad ; \quad M_C = -(\frac{1}{2}+a) b L_C \cos(\varepsilon+\alpha) \\ \text{Where } w_{3/4} = U_a\alpha + \frac{dh}{dt} + (\frac{1}{2}-a)b\frac{d\alpha}{dt} = U_a\alpha + U_\infty\dot{\xi} + U_\infty(\frac{1}{2}-a)\dot{\alpha} \end{gathered} \tag{10}$$

Where ρ is the air density, U_a is the flow approaching velocity, $\phi(\tau)$ is the Wagner's function approximated by R.T. Jones [19,20]. As propeller effects are defined as velocity distributions, U_a is not the same with U_∞.

For non-circulatory lift, they are arised from apparent mass ($\pi\rho b^2$) and can be formulated in dimensionless time domain as

$$\begin{aligned} L_{NC} &= -\pi\rho b U_\infty^2(\ddot{\xi} - a\ddot{\alpha}) - \pi\rho b U_a U_\infty \dot{\alpha} \\ M_{NC} &= \pi\rho a b^2 U_\infty^2(\ddot{\xi} - a\ddot{\alpha}) - (1/2-a)\pi\rho b^2 U_a U_\infty \dot{\alpha} - \frac{1}{8}\pi\rho b^2 U_\infty^2 \ddot{\alpha} \end{aligned} \tag{11}$$

Propellers mounted on the wing not only add weights G_{prop} on wing tips, but also complicate the flow characteristics. As shown in Figure 3, for the propeller-covered area, there are additional velocity in the y-direction, additional velocity in the z-direction and sinusoidal velocity variation in the z-direction.

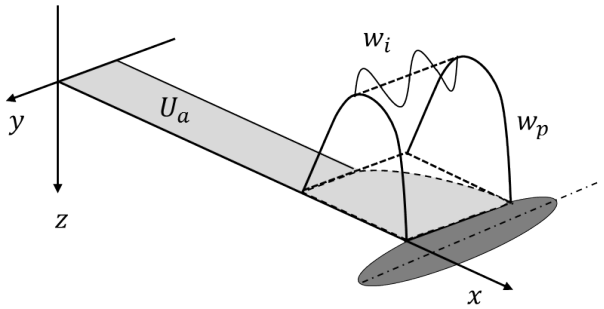

Figure 3: Propeller vertical and axial effects on fixed wing

In the vertical direction, there are several velocity components needed to be taken into consideration for the present study. Firstly, to reproduce effects of the wing's built-in angle (ε_0), a equivalent step-gust ($w_0 = U_a \tan\varepsilon_0$) going through horizontally-placed wing can be used along full length of the wing span. As for the propellers, in the propeller-covered area, a parabolic velocity profile w_p was assumed with sinusoidal variation w_i. Therefore, the total vertical velocity component can be written as Equation (12).

$$w_G(x,\tau) = \begin{cases} w_0(x,\tau) & \text{without propeller} \\ w_0(x,\tau) + w_p(x,\tau) + w_i(x,\tau) & \text{with propeller} \end{cases} \tag{12}$$

Due to the periodical nature of a propeller, the sinusoidal variation w_i regarding to the shear centre can be expressed in dimensionless domain as

$$w_i(x,t) = w_i(x)\sin\omega_p(t - b(1+a)/U_a) \Longrightarrow w_i(x,\tau) = w_i(x)\sin k_p(\tau - U_\infty(1+a)/U_a)$$

Where ω_p is the blade-passing frequency relative to the wing, $k_p = \omega_p b/U_\infty$ is the reduced frequency in the dimensionless time domain.

As Küssner developed a theory characterising aerodynamic loadings exerted in any arbitrary velocity field [21], the lift and moment components can be written as Equation (13). Due to its circulatory nature, L_g shares the same direction with L_C, while M_g shares a similar formulation with M_C.

$$L_g(\tau) = -2\pi\rho b U_a \int_0^\tau w_G(\tau)\frac{\partial\psi(\tau-\tau_0)}{\partial\tau}d\tau_0 \quad ; \quad M_g(\tau) = -(1/2+a)bL_g\cos(\varepsilon+\alpha) \tag{13}$$

Where $\psi(\tau)$ is the Küssner's function approximated by Sears and Sparks [22].

Overall, loadings in the flapping and torsional directions can be written as

$$L_h = (L_C+L_g)\cos(\varepsilon+\alpha)+L_{NC}+D\sin(\varepsilon+\alpha)+G_{prop}\cos\alpha\,;\; M_\alpha = M_C+M_{NC}+M_g-(\frac{1}{2}+a)bD\sin(\varepsilon+\alpha) \tag{14}$$

2.3 Aeroelastic Model

A general matrix form of the governing equation can be obtained by combining the Timoshenko beam model and aerodynamic loadings and then lead to an solution by applying Galerkin's method. Note that there is no added damping for the structure. Any damping effect is originated from aerodynamic loading formulations.

$$\mathbf{M}\ddot{\boldsymbol{u}} + \mathbf{K}\boldsymbol{u} = \boldsymbol{F}$$

$$\text{where} \quad \mathbf{M} = [\mathbf{M_{ij}}]_{N\times N} = \begin{bmatrix} m\int_0^l \theta_i\theta_j dx & 0 & -mx_\alpha\int_0^l \theta_i\eta_j dx \\ 0 & \rho I_y\int_0^l \phi_i\phi_j dx & 0 \\ -mx_\alpha\int_0^l \eta_i\theta_j dx & 0 & I_\alpha\int_0^l \eta_i\eta_j dx \end{bmatrix}_{N\times N}$$

$$\mathbf{K} = [\mathbf{K_{ij}}]_{N\times N} = \begin{bmatrix} -\kappa_h GAb\int_0^l \theta_i\theta_j''dx & \kappa_h GA\int_0^l \theta_i\phi_j'dx & 0 \\ -\kappa_h GAb\int_0^l \phi_i\theta_j'dx & -EI_y\int_0^l \phi_i\phi_j''dx + \kappa_h GA\int_0^l \phi_i\phi_j dx & 0 \\ 0 & 0 & -GJ\int_0^l \eta_i\eta_j dx \end{bmatrix}_{N\times N}$$

$$\ddot{\boldsymbol{u}} = [\ddot{\boldsymbol{u}}_j]_{N\times 1} = \begin{bmatrix} \frac{U_\infty^2}{b}\ddot{q}_j \\ \frac{U_\infty^2}{b^2}\ddot{q}_j \\ \frac{U_\infty^2}{b^2}\ddot{q}_j \end{bmatrix}_{N\times 1} \qquad \boldsymbol{u} = [\boldsymbol{u}_j]_{N\times 1} = \begin{bmatrix} q_j \\ q_j \\ q_j \end{bmatrix}_{N\times 1} \qquad \boldsymbol{F} = [\boldsymbol{F}_i]_{N\times 1} = \begin{bmatrix} \int_0^l \theta_i L_h dx \\ 0 \\ \int_0^l \eta_i M_\alpha dx \end{bmatrix}_{N\times 1} \tag{15}$$

Recursive optimisation was carried out on convolution integral to improve model efficiency, with a linear Newmark-beta integration method implemented, as discussed in [14].

3 Case study parameters

A case resembling a similar short-wing configuration with Eurocopter X3 is studied to investigate the tool's capability. The parameters are presented as Table 2. The propeller velocity distribution are shown in Figure 4.

Table 2: Structural parameters of short wing

Mass m	22.3040 kg/m	Wing built-in angle ε_0	2 deg
Mass moment of inertia I_α	0.4714 kgm^2/m	Aircraft cruising speed U_∞	120 m/s
Bending stiffness EI_y	3.2146$\times 10^5$ Nm^2	Max. advancing speed addition	8 m/s
Torsional stiffness GJ	4.1276$\times 10^5$ Nm^2	Max. vertical velocity addition	7 m/s
Rotary inertia $\rho_w I_y$	0.0127 kgm^2/m	Sinusoidal variation	10%
Shear stiffness $\kappa_h GA$	9.7416$\times 10^7$ N	Blade-passing frequency ω_p	136.5 Hz
Aerofoil chord $c = 2b$	0.6 m	Propeller weight	490.5 N
Wing semi-span l	2.5 m	Lift/drag ratio	1/10
Shear centre offset x_α	0.09 m	Air density	1.225 kg/m^3

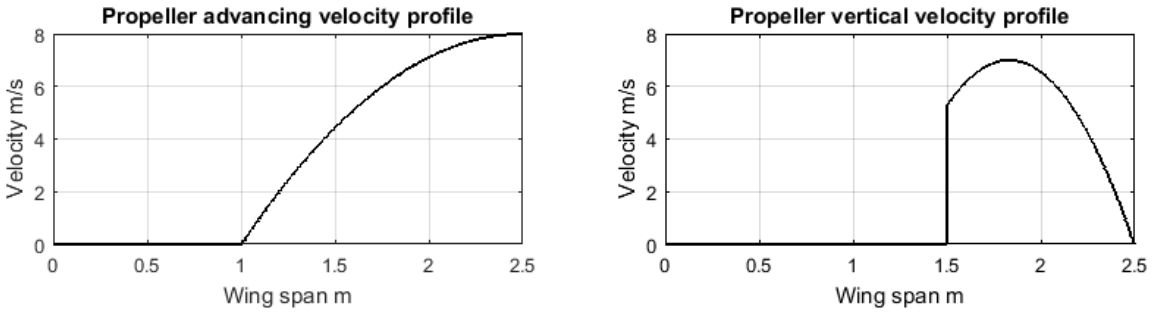

Figure 4: Propeller velocity addition in the y (advancing) and z (vertical) directions

3.1 Shear coefficient determination

For Timoshenko beam, shear coefficient is an important parameter. The shear coefficient κ_h is dependent on the shape of beam cross-section. In many studies, shear coefficients for various of cross-sectional types were approximated or validated. Although most beams have an arbitrary cross-section, simplification can be made in many cases. Standard cross-sections, such as rectangular, circular and hollow, etc. are used. In this case, the wing is simplified as a wing-box section, therefore a thin-wall box section was assigned. According to Cowper's study in [23], shear coefficient for box section is 0.44. This value is implemented in the presented Timoshenko beam model.

3.2 Modal analysis

Based on structural parameters given in Table 2, natural frequencies and their corresponding mode shapes can be investigated . Using modal analysis techniques introduced in Section 2.1.1, modal properties of the given system can be obtained. In Table 3, natural frequencies obtained by uncoupled and coupled approaches are listed and compared. Great differences can be observed from the third mode, especially when torsion is involved.

Uncoupled mode shapes for beam bending and torsion are well established and used for vibration problems. Their analytical expression can be found in many standard books. The coupled mode shapes obtained by transfer matrix method are shown in Figure 5. As illustrated, the first two modes are bending governed

Table 3: Natural Frequency comparisons

Uncoupled approach	Coupled approach	% Difference
10.73 Hz (Bending)	10.71 Hz	0.19%
66.70 Hz (Bending)	65.43 Hz	1.94%
93.57 Hz (Torsion)	120.31 Hz	22.23%
184.27 Hz (Bending)	177.49 Hz	3.82%
280.71 Hz (Torsion)	329.02 Hz	14.68%
354.38 Hz (Bending)	365.40 Hz	3.02%

with little torsion involvement. From the 3rd mode onwards, coupled behaviour in bending and torsion starts to show. The third and forth modes are torsion governed with considerable amount of bending and sectional rotation involved. While for the fifth and sixth modes, they are governed by sectional rotation, with considerable bending and torsion behaviour.

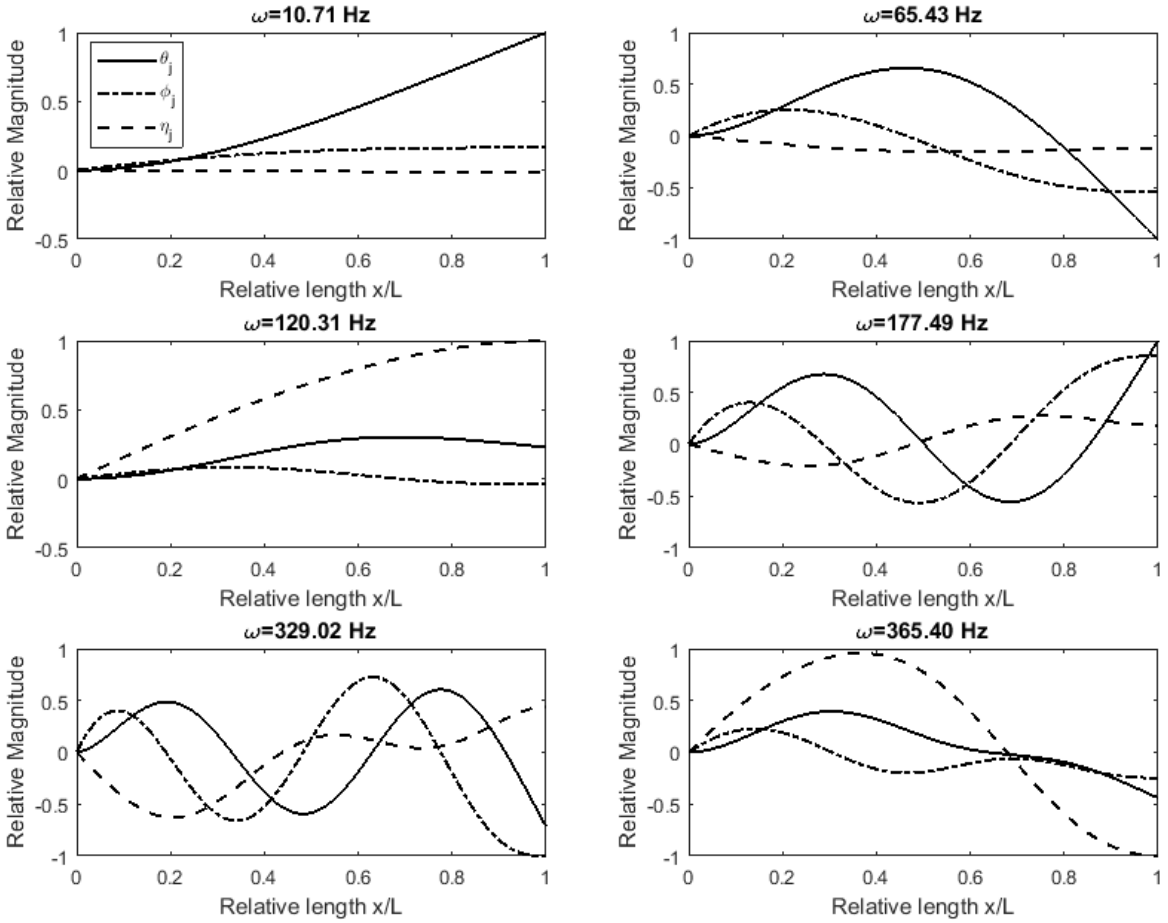

Figure 5: Coupled modal frequencies and shapes

3.3 Convergence study

A convergence study is carried out to determine the minimum number of modes to include and the maximum iterative time step. Steady-state vibrating amplitudes are compared with different number of modes and time step sizes. A 5% difference is considered as convergence. Detailed convergence study procedures can be found in [14]. In the case studied, five coupled modes is considered and iterative time step is taken as 1/8 of the smallest natural period involved.

4 Results and discussions

Aeroelastic responses of a short wing undergoing constant cruising velocity and an operating propeller is simulated to demonstrate capabilities of the numerical model. Transient and steady-state responses are shown and compared with the ones obtained by uncoupled modes, also with results based on the Euler-Bernoulli beam theory.

Comparing aeroelastic responses captured via coupled and uncoupled analytical mode shapes, an illustration is shown in Figure 6. For both methods, a similar transient response is shown. For the steady states, again, these two approaches gave very similar responses. However, differences can be observed for the transient and steady-state amplitudes. In the transient regime, coupled modes gave a slightly larger deflection compared to results from uncoupled modes. As for the steady states, 2.5% and 6.8% differences in amplitude are found between coupled and uncoupled mode shapes for bending and torsion respectively. However, vibrating amplitudes are less than 1% of the overall deflections. Therefore, they are insignificant for the overall steady-state behaviours. More importantly, by using coupled mode shapes, computational time is reduced. For uncoupled mode shapes, each vibration mode shape has one time-dependent function. While for coupled modes, one time-dependent function is shared between three mode shape functions. This reduces the number of variables by three, hence reduces the computational power needed. For solving the presented case with a standard desktop PC, using coupled modes can reduce the program operation time by 30%.

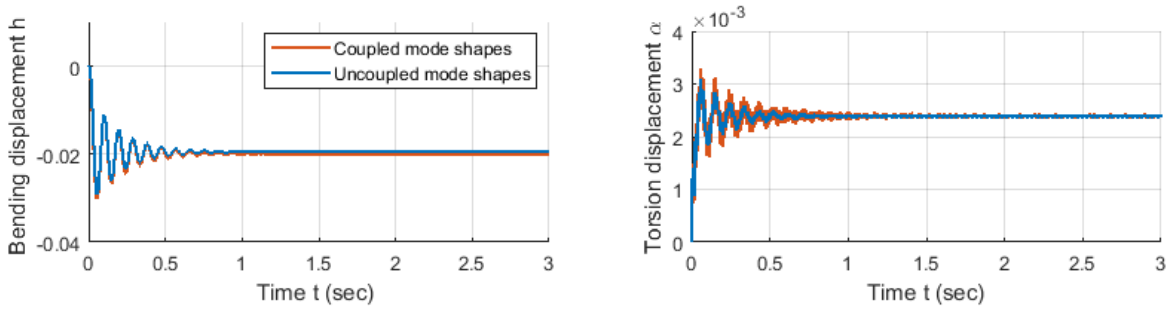

Figure 6: Coupled/Uncoupled transient response comparison (left: bending, right: torsion)

Table 4: Uncoupled/coupled mode shape steady-state response comparison

	Uncoupled	Coupled	% Difference
Bending mean deflection	0.01946 m	0.01995 m	2.5%
Bending amplitude	1.981e-06 m	1.952e-06m	1.5%
Torsional mean deflection	0.002387 rad	0.002390 rad	0.1%
Torsional amplitude	2.550e-5 rad	2.735e-5 rad	6.8%

Figure 7 shows the aeroelastic responses given by Euler-Bernoulli and Timoshenko beam theories. Two methods showed an extremely similar transient response and a very close steady state, according to Table 4. Therefore, for this case, the rotational and shear deformation effects are not significant. When use Euler-Bernoulli beam theory, sectional rotation is constrained to be perpendicular to the neutral axis. This coupling stiffens the structure [10]. While for the Timoshenko beam, bending and rotational coupling can be avoided, making the beam more flexible and resulting in a greater steady-state bending deflection. However, due to energy conservation, while having a smaller mean deflection, Euler-Bernoulli beam model has a greater vibration amplitude in bending. As for torsion, stiffness remains the same for Timoshenko and Euler-Bernoulli beams, therefore, the steady-state mean deflection is nearly identical. The amplitude differences in bending, however, propagated into its torsional behaviour, resulting in a difference of just below 10%. This revealed a different energy distribution mechanism when rotary inertia and shear deformations are considered in the presented aeroelastic system.

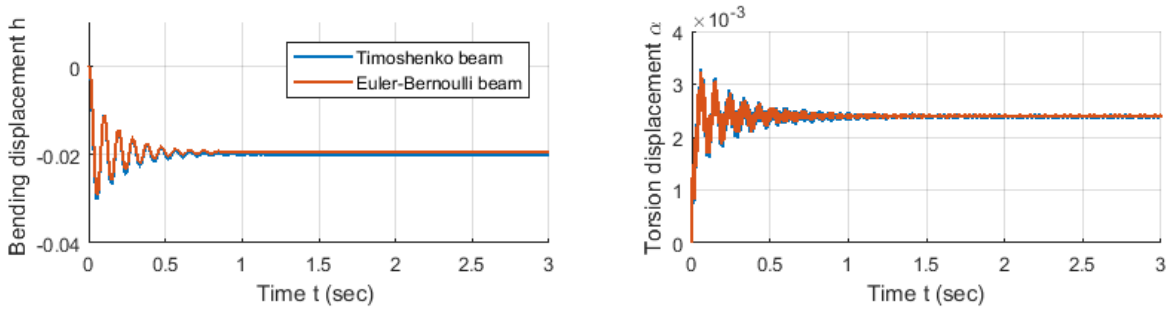

Figure 7: Timoshenko / Euler-Bernoulli response comparison

Table 5: Steady-state response comparison

	Euler-Bernoulli	Timoshenko	% Difference
Bending mean deflection	0.019402 m	0.019947 m	2.7%
Bending amplitude	2.146e-6 m	1.952e-6 m	9.9%
Torsional mean deflection	0.002398 rad	0.002390 rad	0.3%
Torsional amplitude	2.487e-5 rad	2.735e-5 rad	9.1%

5 Conclusion

This paper has presented a simplified numerical model based on a short and bending-torsion coupled structure in cruising and propeller inflow. Focusing on the application of coupled modal analysis and Timoshenko beam theory in an aeroelaticity context, a case similar to the Eurocopter X3 short-wing/propeller configuration has been studied for its time-domain response. Differences in aeroelastic response introduced by coupled mode shapes and Timoshenko beam theory are analysed and discussed. In general, the steady-state response given by uncoupled and coupled approach are similar. However, with the coupled modal analysis approach, a more realistic modal behaviour can be captured with less computational power. Also, it is compatible with complex structural models, allowing stiffness, material, geometry or any other cross-sectional property variations along the wing span to be considered. Hence, its advantages over uncoupled modal analysis approach will appear further as complex structures and more modes are included. As for the implementation of Timoshenko beam, its response is not significantly different compared to Euler-Bernoulli beam. However, Timoshenko beam showed that the rotary inertia and shear deformations affect how energy is distributed in the steady state, giving a larger mean deflection and a smaller vibration amplitude in the flapping coordinate, revealing a different energy distribution mechanism in the aeroelastic system studied.

Acknowledgements

The work of ZW is partially supported by EU Clean Sky 2 Joint Undertaking ASTRAL project.

References

[1] A. Mazidi, H. Kalantari, and S. A. Fazelzadeh, "Aeroelastic response of an aircraft wing with mounted engine subjected to time-dependent thrust," *Journal of Fluids and Structures*, vol. 39, pp. 292–305, 2013.

[2] S. Shams, M. H. Sadr Lahidjani, and H. Haddadpour, "Nonlinear aeroelastic response of slender wings based on Wagner function," *Thin-Walled Structures*, vol. 46, no. 11, pp. 1192–1203, 2008.

[3] M. J. Patil and D. H. Hogdes, "Limit-Cycle Oscillations in High-Aspect-Ratio Wings," *Journal of Fluids and Structures*, vol. 16, no. 15, pp. 107–132, 2001.

[4] S. Preidikman, "Numerical Simulations of Interactions Among Aerodynamics, Structural Dynamics, and Control Systems," Ph.D. dissertation, Virginia Polytechnic Institute and State University, USA, 1998.

[5] T. W. Strganac, "A Numerical Model of Unsteady, Subsonic Aeroelastic Behavior," Ph.D. dissertation, Virginia Polytechnic Institute and State University, USA, 1987.

[6] M. Gennaretti, M. Molica Colella, and G. Bernardini, "Prediction of tiltrotor vibratory loads with inclusion of wing-proprotor aerodynamic interaction," *Journal of Aircraft*, vol. 47, no. 1, pp. 71–79, 2010.

[7] D. H. Hodges and R. A. Ormiston, "Stability of elastic bending and torsion of uniform cantilever rotor blades in hover with variable structural coupling," NASA, Tech. Rep. D-8192, 1976.

[8] D. H. Hodges and E. H. Dowell, "Nonlinear equations of motion for the elastic bending and torsion of twisted nonuniform rotor blades," NASA, Tech. Rep. D-7818, 1974.

[9] M. Berci, P. H. Gaskell, R. W. Hewson, and V. V. Toropov, "A semi-analytical model for the combined aeroelastic behaviour and gust response of a flexible aerofoil," *Journal of Fluids and Structures*, vol. 38, pp. 3–21, 2013.

[10] M. Kämpchen, A. Dafnis, H. G. Reimerdes, G. Britten, and J. Ballmann, "Dynamic aero-structural response of an elastic wing model," *Journal of Fluids and Structures*, vol. 18, no. 1, pp. 63–77, 2003.

[11] J. R. Banerjee, "Explicit Frequency Equation and mode shapes of a centilever beam coupled in bending and torsion," *Journal of Sound and Vibration*, vol. 224, no. 2, pp. 267–281, 1999.

[12] ——, "Explicit modal analysis of an axially loaded timoshenko beam with bending-torsion coupling," *Journal of Applied Mechanics*, vol. 67, no. 2, pp. 307–313, 2000.

[13] J. R. Banerjee and H. Su, "Free transverse and lateral vibration of beams with torsional coupling," *Journal of Aerospace Engineering*, vol. 19, no. 1, pp. 13–20, 2006.

[14] Z. Wang, A. Anobile, and A. A. Popov, "Efficient numerical methods for aeroelastic analysis of wing-propeller configuration compound helicopters," in *XXIV A.I.D.A.A. Conference*, Palermo, Italy, 2017.

[15] ——, "Time-domain aeroelastic model for compound helicopter propeller-wing configuration," in *Aerospace Europe 6th CEAS Conference*, Bucharest, Romania, 2017.

[16] S. Timoshenko, "On the correction factor for shear of the differential equation for transverse vibrations of bars of uniform cross-section," *Philosophical Magazine*, vol. 41, pp. 744–746, 1921.

[17] ——, "On the transverse vibrations of bars of uniform cross-section," *Philosophical Magazine*, vol. 43, pp. 125–131, 1922.

[18] H. Wagner, "Über die Entstehung des dynamischen Auftriebes von Tragflügeln," *Zeitschrift für angewandte Mathematik and Mechanik*, vol. 5, no. 1, pp. 17–35, 1925.

[19] R. T. Jones, "Operational treatment of the nonuniform-lift theory in airplane dynamics," NACA, Tech. Rep. 667, 1938.

[20] ——, "The unsteady lift of a wing of finite aspect ratio," NACA, Tech. Rep. 681, 1940.

[21] H. G. Küssner, "Zusammenfassender Bericht über den instationären Auftrieb von Flügeln," *Luftfahrtforschung*, vol. 13, no. 12, pp. 410–424, 1935.

[22] W. Sears and B. Sparks, “On the reaction of an elastic wing to vertical gusts,” *Journal of the Aeronautical Sciences*, vol. 9, no. 2, pp. 64–67, 1941.

[23] R. G. Cowper, “The Shear Coefficient in Timoshenko’s Beam Theory,” *Journal of Applied Mechanics*, vol. 33, pp. 335–340, 1966.